Theoretical Studies on the Beam Position Measurement with Button-type Pickups in APS*

Y. Chung
Argonne National Laboratory
9700 S. Cass Ave., Argonne, IL 60439

Abstract

The response of electrostatic button-type pickups for the measurement of the transverse position of charged particle beams was investigated and analytical formulae were obtained for the signal as a function of time t and the coordinates of the beam and the electrodes. The study was done for beam pipes of circular and elliptic cross sections, for rectangular and non-rectangular electrodes, and for several cases of longitudinal beam profiles. The numerical results show good agreement with the analytical results, except that the presence of the photon beam channel and the antechamber causes finite offset (~20 μm) of the electrical center in the horizontal direction. Time domain analysis indicates that the error in the measurement of the beam position using circular electrodes as compared to rectangular ones was found to be less than 100 μm per 1 cm of beam excursion from the center of the beam pipe for the case of APS storage ring vacuum chamber.

I. INTRODUCTION

For capacitive pickup devices[1-3], the position of the charged beam is measured through the difference between the electric potentials which develop on the electrodes. For highly relativistic beams, the image charge has the same longitudinal distribution as the beam, due to the Lorentz contraction of the longitudinal component of the electric field.

In this article, we will analyze the response of the button electrodes in both the frequency and the time domains as a function of the transverse position of the beam, taking into account the finite size of the electrodes. The analytical model assumes a simple elliptic geometry for the beam chamber. The results are compared with those obtained numerically for the actual APS beam chamber, and they will be shown to agree quite well. This justifies the use of the analytical model rather than the time-consuming numerical methods to find the optimal position and size of the electrodes and to analyze how the shape of the electrodes affect the beam position measurement.

II. MONITOR RESPONSE

Consider an infinitely narrow beam moving along the longitudinal direction with the constant velocity V. Following the procedure by Cupérus[4], instead of solving the full electromagnetic problem directly in the lab frame (unprimed), we will transform to the reference frame (primed) where the beam is at rest, obtain the field and then transform back to the lab frame. The electric field $\mathbf{E}$ in the lab frame is then, using the Lorentz transformation,

$$E_{\|} = E'_{\|}, \qquad \text{and} \qquad \mathbf{E}_{\perp} = \gamma \mathbf{E}'_{\perp}, \tag{1}$$

where $\gamma = (1 - V^2/c^2)^{-1/2}$. Thus, the problem is reduced to that of an electrostatic case with linearly distributed charges.[5]

We will first concentrate on the frequency domain, and then discuss the solution in the time domain. Decomposing the electric potential $\Phi'(\mathbf{x}, t)$ into Fourier components, we write

$$\Phi'(\mathbf{x}, t) = \int dk\, e^{ik(z - Vt)}\, \Phi'(\mathbf{x}_{\perp}, k), \tag{2}$$

where the linear dispersion relation $\omega = kV$ was assumed. The integration variable k extends from $-\infty$ to $+\infty$. Then the induced current I_p can be expressed as

$$I_p(k) = i\gamma\varepsilon_0 kV \int dS\, e^{ik(z - z_1)} \frac{\partial \Phi'(\mathbf{x}_{\perp}, k)}{\partial n}. \tag{3}$$

The integration is done over the area of the electrode surface, and z_1 is the z-coordinate of a reference point, e.g., the center of the electrode z_p. $\mathbf{n}$ is the direction normal to the electrode surface. If the electrode is connected by a coaxial line of characteristic impedance Z_0 and if the capacitance between the electrode and the beam chamber is C_p, then the overall impedance $Z_p(k)$ for the electrode will be

$$Z_p(k) = \left(\frac{1}{Z_0} - ikVC_p\right)^{-1}. \tag{4}$$

If there is frequency filtering represented by F(k), the measured voltage $V_p(k)$ will be

$$V_p(k) = Z_p(k)\, I_p(k)\, F(k). \tag{5}$$

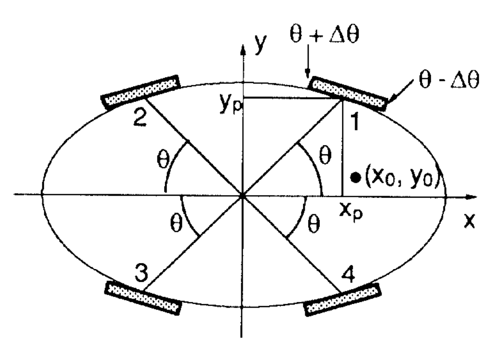

Fig. 1: Geometry of the beam chamber and the pickup electrodes.

---
*Work supported by the U.S. Department of Energy, Office of Basic Energy Sciences, under Contract No. W-31-109-ENG-38.

From Eqs. (3) and (5), it suffices to solve the Poisson equation for the 2-D static potential $\Phi'(\mathbf{x}_\perp, k)$ to obtain the electrode response V_p. The equation is analytically solvable if the beam chamber geometry is somewhat simplified. In this work, elliptic coordinates will be used to approximate the APS beam chamber. We will consider highly relativistic beams only. The current I_b carried by the beam is represented by

$$I_b(k) = \frac{Q_b V D(k)}{2\pi}, \qquad D(0) = 1. \tag{6}$$

Q_b is the total charge in a single bunch and D(k) is the Fourier transform of the longitudinal charge distribution $\rho(z)$.

Assuming a rectangular electrode flush with the interior surface, the electrode current $I_p(k)$ can be expressed as

$$I_p(k) = -i\frac{2\Delta\theta}{\pi} I_b(k) \sin k\Delta z \, G(\mu_0, \theta_0), \tag{7}$$

where

$$G(\mu_0, \theta_0) = 1 + 2\sum_{m=1}^{\infty} \frac{\sin m\Delta\theta}{m\Delta\theta} G_m(\mu_0, \theta_0), \tag{8}$$

and

$$G_m(\mu_0, \theta_0) = \frac{\cosh m\mu_0}{\cosh m\mu_p} \cos m\theta_0 \cos m\theta_p + \frac{\sinh m\mu_0}{\sinh m\mu_p} \sin m\theta_0 \sin m\theta_p. \tag{9}$$

Here, $\Delta\theta$ and Δz are half the angular and the longitudinal sizes of the rectangular electrode. The subscripts 0 and p denote the bunch and the electrode, respectively. From Eqs. (5) and (7), the coupling impedance $Z_c(k)$ can be obtained:

$$Z_c(k) = \frac{V_p(k)}{I_b(k)} = -i\frac{2\Delta\theta}{\pi} \sin k\Delta z \, G(\mu_0, \theta_0) \, Z_p(k) \, F(k). \tag{10}$$

In the time domain, we find from Eq. (5) that $V_p(t)$ is separated into the time-dependent and the position-dependent factors for rectangular electrodes as

$$V_p(t) = T(t) \, P(\mathbf{x}_{\perp 0}), \tag{11}$$

where

$$T(t) = \frac{Q_b \Delta\theta}{\pi^2 C_p} \int dk \, \frac{e^{ik(z_1 - Vt)}}{k + i\kappa} \sin k\Delta z \, D(k) \, F(k),$$

$$\left(\kappa = \frac{1}{Z_0 V C_p}\right) \tag{12}$$

and

$$P(\mathbf{x}_{\perp 0}) = P_0(\mathbf{x}_{\perp 0}) + \sum_{m=1}^{\infty} \frac{\sin m\Delta\theta}{m\Delta\theta} P_m(\mathbf{x}_{\perp 0}). \tag{13}$$

For the elliptic case,

$$P_m(\mathbf{x}_{\perp 0}) = \frac{2}{1 + \delta_{m0}} G_m(\mu_0, \theta_0). \tag{14}$$

Once the longitudinal charge distribution $\rho(z)$ and the filtering function F(k) are known, it is straightforward to calculate the electrode response $V_p(t)$. For certain cases of $\rho(z)$, it is possible to evaluate $V_p(t)$ analytically using the residue theorem of complex variables. In the discussion below, we will use the following parameters: $C_p = 6$ pF, $\Delta z = 0.5$ cm, $\sigma = 1$ cm, $Q_b = 3.5$ nC / mA (single bunch), $x_p = 1.38$ cm. Figure 2 shows the electrode signal $V_p(t)$ without frequency filtering. If the electrodes are not rectangular, the results are similar but a bit more complicated. One notable difference is that $V_p(t)$ for non-rectangular electrodes is not separable as in Eq. (11).

III. Beam Position Measurement

As shown in Fig. 1, four button-type pickups will be installed for each unit. The quantities Δ_x, Δ_y and Σ are defined as follows.

$$\begin{aligned} \Delta_x &= V_{p1} + V_{p4} - V_{p2} - V_{p3}, \\ \Delta_y &= V_{p1} + V_{p2} - V_{p3} - V_{p4}, \\ \Sigma &= V_{p1} + V_{p2} + V_{p3} + V_{p4}. \end{aligned} \tag{15}$$

The horizontal and the vertical positions of the beam are then determined from

$$X_0 = \frac{\Delta_x}{\Sigma} \approx S_x x_0 + R_x, \text{ and } Y_0 = \frac{\Delta_y}{\Sigma} \approx S_y y_0 + R_y. \tag{16}$$

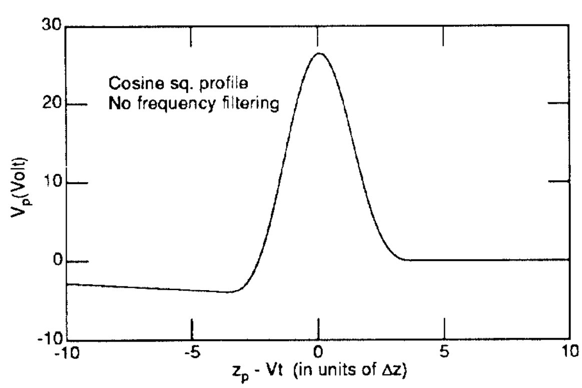

Fig. 2: The electrode signal V_p as a function of time t without frequency filtering. z_p is the electrode center coordinate and Δz is half the longitudinal size.

	Analytical result	Numerical result	
y_0 (cm)	S_x (cm^{-1})	S_x (cm^{-1})	R_x
0.0	0.569	0.565	-0.0011
0.2	0.580	0.576	-0.0011
0.4	0.616	0.610	-0.0011
0.6	0.676	0.667	-0.0010
0.8	0.763	0.747	-0.0010
1.0	0.877	0.850	-0.0009
1.2	1.017	0.974	-0.0008
1.4	1.178	1.113	-0.0008

Table 1: Comparison between the analytical and the numerical results for the x direction. The offset R_x for the analytical case is zero.

The linear approximation is valid only when x_0 and y_0 are small. S_x and S_y are the sensitivity functions and R_x and R_y are the offset errors. Figure 3 shows X_0 as a function of the beam position x_0 for several cases of y_0, and Fig. 4 shows the contour plotting of both X_0 and Y_0. Table 1 lists the sensitivity function S_x obtained analytically for the elliptic beam chamber and numerically for the actual APS beam chamber. The two results agree quite well. The finite offset error R_x is due to broken symmetry in the x-direction due to the presence of the photon beam channel and the antechamber. The optimal position of the electrodes which gives the same sensitivity in both x and y directions was found to be x_p =

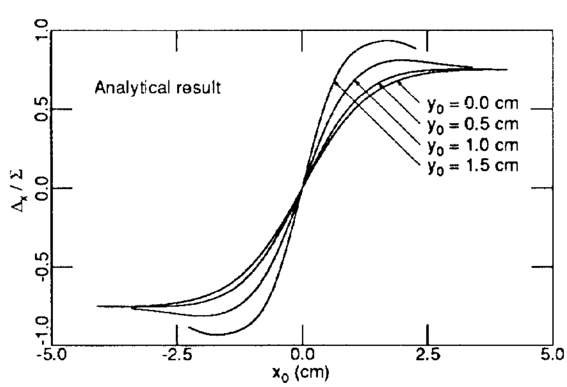

Fig. 3: The ratio Δ_x/Σ as a function of the beam position x_0 for several cases of y_0.

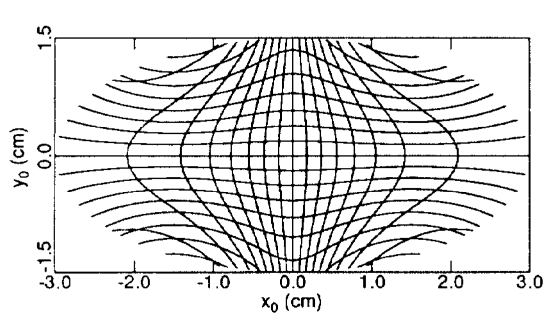

Fig. 4: The contour plotting for $X_0 = \Delta_x/\Sigma$ and $Y_0 = \Delta_y/\Sigma$ for the elliptic beam chamber.

1.32 cm. However, this was shifted to x_p = 1.38 cm due to the mechanical constraint of the mounting flanges.

If the electrodes are not rectangular, X_0 and Y_0 are time-dependent, and the result of measurement will depend on the timing of data acquisition. This error due to the timing jitter will be larger for wide-band detection than for narrow-band detection at low frequency, say, a few hundred MHz. The measurement error can be expressed as

$$\delta x_0 = - \frac{\delta S_x(t)}{S_x(t)} x_0. \tag{17}$$

$S_x(t)$ is the sensitivity as a function of time. Using hexagonal electrodes in place of circular ones to facilitate analytic integration over the electrode surface, typical error is found to be less than 100 μm per 1 cm of beam excursion from the beam chamber center. It is to be noted that it will diverge to infinity when Σ crosses zero while Δ_x does not. If the timing jitter is small (less than 10 ps) or if a narrow band detection scheme at a few hundred MHz is used, this error will be reduced to a negligible level (less than 10 μm / cm).

IV. CONCLUSION

The characteristic of the BPM system for the APS storage ring was studied analytically and numerically, and the results agree very well. This suggests that the presence of the photon beam BPM system. Using the analytical model, the optimal position of the electrodes was determined such that the sensitivity is as close as possible in x and y directions taking into account other mechanical constraints. A possible source of error in the measurement of the beam position using non-rectangular electrodes was analyzed. The error was found to be typically of the order of 100 μm per 1 cm of beam excursion from the center of the beam chamber and can be reduced significantly by employing proper timing schemes and signal processing.

V. REFERENCES

[1] T. Ring, "Beam Position Monitors for the High Brightness Lattice," Daresbury Laboratory Report, DL/SCI/TM41A, 1985

[2] J. Hinkson, J. Johnson, and I. Ko, "Advanced Light Source (ALS) Beam Position Monitor," *Proceedings of 1989 IEEE Particle Accelerator Conference*, 1507, 1989

[3] J.-C. Denard, A. Carniel, R. Aiello, and T. Monaci, "Beam Position Monitoring System for Elettra," *Proceedings of 1990 European Particle Accelerator Conference*, 726, 1990

[4] J. H. Cupérus, "Monitoring of particle beams at high frequencies," Nucl. Instr. and Meth. **145**, 219, 1977.

[5] J. Borer and C. Bovet, "Computer Response of Four Pick-up Buttons in an Elliptical Vacuum Chamber," LEP Note 461, 1983, and references therein